Response to reviewer 1 comments

In the manuscript "Long-range transport of Canadian Wildfire smoke to Europe in Fall 2023: aerosol properties and spectral features of smoke particles", Masoom et al., present a multi-instrument study of a long-range smoke transport event originating from Canadian wildfires in late September–early October 2023. Using ground-based column (AERONET, PFR, spectroradiometers) and in-situ (JFJ) measurements, lidar/ceilometer profiles, satellite imagery (MODIS) and HYSPLIT back-trajectories, they document an unusual concave spectral AOD (AOD peaking near ~500 nm) and associated optical/microphysical signatures: very large accumulation-mode volume median diameters (VMDs up to ~800 nm), high UV absorption (AAE ≈ 2), and non-monotonic single-scattering albedo (SSA) spectra. They use Mie calculations to show that the AOD curvature is primarily a scattering/size effect given the retrieved refractive indices. The observations are interesting and important for understanding extreme wildfire aerosol radiative effects and long-range plume evolution. Also, the work is timely, given increasing wildfire activity under climate change, and provides valuable observational evidence of an infrequently occurring and intriguing smoke event. However, several key aspects require clarification, deeper mechanistic explanations, and improved discussion of uncertainties. Below, I outline major and minor concerns:

General Comments:

Comment #1: The manuscript attributes the large particle sizes (~800 nm) to 'low dilution' and 'high VOC concentrations,' but would benefit from more quantitative analysis of growth pathways (coagulation, condensation, SOA formation). The non-monotonic SSA spectral curvature may additionally reflect evolving aerosol mixing states during aging, as demonstrated in other environments with complex aerosol mixtures. Recent studies of biomass burning and urban aerosols in South/Southeast Asia (Tiwari et al., 2023, 2025; Liu J et al., 2024) have revealed similar particle sizes occurring through secondary processes under favorable aging conditions. The resulting core-shell mixing states produce comparable non-monotonic SSA spectral curvature patterns through coating-dependent absorption enhancement. These studies provide valuable mechanistic frameworks that could help test whether similar growth pathways operate in boreal wildfire plumes, interpret the unique DAV/JFJ SSA behavior through mixing-state analogs and strengthen the global context by showing these processes transcend source regions. Incorporating such cross-comparisons would demonstrate how localized observations fit into broader patterns of aerosol evolution. These works also make clear that while such a non-monotonic SSA spectra is infrequent, it has been observed in previous work in other parts of the world, and also associated with urban pollution plumes as well as fire pollution plumes.

Response #1: We thank the reviewer for this comment and making us aware of the mentioned recent studies.

In order to have a global comparison, we have included a description about the observation of non-monotonic SSA around the world from relevant previous studies as mentioned in Lines 455-463 and described below

"For dust particles, the SSA typically monotonically increases with wavelengths (Li et. al., 2015; Collaud Coen et al., 2004; Yus-Díez et al., 2021; Kaskaoutis et al., 2021) whereas for black carbon dominated absorbing aerosols, the SSA usually monotonically decreases with wavelength (Li et. al., 2015; Chauvigné et al., 2019; Kaskaoutis et al., 2021). However, nonmonotonic spectral curvature in SSA is dominant in East Asia, peaking at 675 nm, as reported by Li et. al. (2015) and attributed to enhanced absorption by some dust aerosol species in the UV region that become non-absorbing in the visible part of the spectrum and black carbon dominant absorption at longer wavelengths. The uniqueness of the case in the present manuscript is that similar nonmonotonic spectral SSA curvature occurred under conditions of large submicron particles with narrow size distribution (as presented in Fig. 4 and Fig. 6)."

The quantitative analysis of growth pathways (coagulation, condensation, SOA formation) are out of the scope of the current manuscript, however it can be looked into in future work. We have mentioned this in the conclusion section in Lines 710-711 as

"Future investigation can be made on a quantitative analysis of growth pathways such as coagulation, condensation, and secondary organic aerosol formation for such rare atmospheric observations."

As mentioned by the reviewer, the core-shell mixing states produce comparable non-monotonic SSA spectral curvature patterns through coating-dependent "absorption" enhancement. However, in the present manuscript the observed high SSA values of the aerosol sample presents the evidence that the extinction is primarily driven by scattering in this case as we have further explained in Response #3.

Comment #2: The merging of APS and Fidas size distributions assumes an effective density of 1.6 g cm^{-3} to convert aerodynamic diameter to mobility diameter. Given the extreme accumulation-mode sizes observed (VMD ~800 nm), how sensitive are the merged distributions to this density assumption, particularly for particles approaching 1 μm where dynamic shape factors may become significant? Were any cross-validation measurements performed (e.g., with aerodynamic aerosol classifiers or DMA-CPMA systems) to confirm the accuracy of the merged size distribution in this unusual size regime? Could the near-absence of coarse mode particles (>1 μm) in the merged data potentially reflect artifacts in the APS-Fidas integration method for such large accumulation-mode particles?

Response #2: We thank the reviewer for this comment following which we have added the following description:

The MPSS, APS, and Fidas instruments were operated according to the GAW, ACTRIS, and NABEL network requirements, which include regular sizing checks with monodisperse sizing standards. To represent some of the uncertainty in the merged size distributions in the coarse mode size range where both APS and Fidas measurements were available, we considered the range formed by these two measured distributions. This range is represented by the shaded region in Figure 4. As the reviewer pointed out below, we failed to explain this in our original submission, and we apologize for this oversight. We have added a description of the shaded region to the caption of Figure 4 as explained in our response to the reviewer's comment below.

"The assumed effective density affects one edge of the shaded region in Fig. 4. The position of this edge along the x-axis depends on 1/sqrt(effective density). Therefore, varying the effective density only shifts the edge slightly to the left or right, which has minor influence on the position of the dominant size

distribution mode centered at ~800 nm in the volume size distribution. We place a high degree of confidence in the measurement of this mode, as well as the measurements of relatively low coarse mode particle (Dp>1um) concentrations, because they were obtained independently by two instruments with different operating principles (aerodynamic sizing in the APS, optical sizing in the Fidas)."

We have added the following statement to the revised manuscript to explain these points in Section 2.1.2 in Line 216-217

"The limits formed by the APS and Fidas size distributions around their averages were retained as an indication of the uncertainty in the merged size distributions above 0.6 µm diameter".

and in Section 3.1.3 Line 361-364:

"The presence and location of this large accumulation mode, as well as the relatively lower coarse mode particle concentrations (diameter > 1000 nm), are confirmed by two independent sizing measurements (aerodynamic sizing in the APS, optical sizing in the Fidas), demonstrating a high degree of confidence in these results".

Comment #3: The Mie calculations assume homogeneous spheres with a single refractive index from AERONET inversions. While this simplifies the analysis, it does not explicitly represent coated BC or other heterogeneous morphologies that are expected in aged wildfire smoke. These fires will have a mixture of fresh (irregularly shaped BC), and also rapidly aged BC (coated by non absorbing aerosols, like sulfate or nitrate). If such particles were present, core–shell or externally mixed Mie model could produce different spectral responses, potentially affecting the interpretation of the AOD curvature. It will be difficult for the authors to analyze for both homogenous spheres, fractals and irregular (using DDA, T-matrix approach), but it should be mentioned in the discussion, where the method may not be fully capture these effects, although they still present a formidable representation for the aged aerosols.

Response #3: Thank you very much for this comment.

The optical properties of internally mixed BC fractal aggregates are indeed more complicated than those of simple homogeneous spheres. A more explicit representation of BC morphology and mixing state would certainly be required if one was investigating light absorption aspects more specifically: for example, if one was attempting to calculate the degree of BC absorption enhancement due to the so-called lensing effect, or if one was performing a closure study on measured and calculated SSA. However, in this case we are concerned with total light extinction and its spectral behavior (whether measured as AOD or calculated as extinction coefficients). The in-situ measurements show that the mass fraction of BC in this plume was low, ~3-5%, and that absorption coefficients (due to BC and BrC absorption) were much lower than corresponding scattering coefficients, resulting in high SSA values, ~0.95 (e.g., see Table A1). This means that total light extinction was dominated by light scattering and was relatively insensitive to absorption. This is discussed in Section 3.1.3 with respect to Figs. 5 a) b) and c), which show that the shapes of the extinction spectral profiles are determined by those of the scattering curves, and not the corresponding absorption curves. It is also confirmed by our sensitivity tests for varying effective imaginary RI, as described but not shown in the main text (line 347). Given this insensitivity to the shape of the absorption spectral profile, we refrained from performing more complicated calculations with explicit representations of BC, since they cannot help to explain the curvature in the spectral extinction profile.

While responding to this comment we realized the discussion of Fig. 5 in Section 3.1.3 was based on an earlier version of the figure. We apologize for this mistake and any confusion that it caused. We have updated the text to make the text consistent with the figure. The caption of Figure 5 now states:

"Absorption (a), scattering (b), and extinction (c) spectral profiles calculated at three points during the peak of the plume using Mie theory and the assumption of homogeneous spheres with size distributions constrained by the in situ measurements and a single, effective refractive index given by the corresponding AERONET retrieval. Panels (d), (e), and (f) show the absorption, scattering and extinction profiles, respectively, of monodisperse homogeneous spheres of various sizes, to assess the sensitivity of these profiles to particle diameter. Panels (g), (h), and (i) show the same curves on a linear y-axis".

In addition, we have added the following in Section 3.1.3 in Line 382-388 to respond directly to the reviewer's comment:

"Given the high SSA of the aerosol sample, it is not surprising that extinction is primarily driven by scattering. This observation justifies our choice of the assumption of homogeneous sphere model for calculation of these optical properties, since most particles contributing to the scattering are likely to be well represented by this assumption. It should be noted that if one wished to perform more accurate calculations of the absorption profiles, one would need a model with a more explicit representation of particle morphology and mixing state to account for the presence of internally mixed BC aggregates, which contribute substantially to the measured absorption but only ~3-5% to the total particle mass in the plume. We refrain from such calculations in this manuscript since we are primarily interested in the spectral profiles of total particle extinction and AOD".

Comment #4: The manuscript contains high-quality instrumentation with calibration statements (e.g., QASUME and PFR uncertainty statements), but the uncertainty bounds are not consistently propagated into the main conclusions, provide quantified uncertainties for (a) spectral AOD at key wavelengths, (b) AERONET inversion outputs used (VSD, RI, SSA, AAOD), and (c) in-situ scattering/absorption coefficients. Discuss whether the observed concave spectral curvature (AOD peak at ≈500 nm) is significant given measurement and retrieval uncertainties. Include error bars / shading on the key plots or an appendix table with uncertainty ranges.

Response #4: We thank the reviewer for this suggestion. We have added uncertainty information associated with the dataset used in this manuscript in Section 2.1.1 as below,

1. For remote sensing retrievals:

For AERONET data in Line 149-164:
"The AERONET field instruments are inter-calibrated at Mauna Loa and Izana Langley calibrated reference instruments resulting in AOD uncertainty at optical airmass 1 of ~0.01 in the visible and near infrared increasing to ~0.02 in the UV wavelengths (Eck et al. 1999). The nominal uncertainty in AERONET SSA for AOD at 440 nm above 0.40 is ~0.03 and the SSA uncertainty decreases with increase in AOD (Dubovik et al., 2000; Sinyuk et al., 2020). The estimated uncertainty for real refractive index is well below 0.04 for AOD greater than 0.5 for biomass burning cases (Dubovik et al., 2000; Sinyuk et al., 2020). The uncertainty in volume median radius is estimated to be 0.1$\pm$0.5 % and 5.4$\pm$4 % for fine and coarse mode, respectively (it is an indication of good confidence in size distribution retrievals) (Sinyuk et al., 2020). The absorption

AOD values as reported in the AERONET almucantar inversion dataset are obtained using the relationship AAOD=(1−SSA) ×AOD. A detailed uncertainty estimation of AERONET inversion product for version 3 can be found at Sinyuk et al. (2020). For the analysis in this manuscript, we have used the AERONET inversion products Level 2.0 and Level 1.5 (with sky error below 5% and solar zenith angle above 45° and the coincident AOD values at 440 nm above 0.40)"

For GAWPFR data in Line 169-170:
"Instruments are calibrated yearly or in 2 years on the basis of instrumental and logistic aspects and the calibration uncertainty is assured to be within ±1% (Kazadzis et al., 2018a)."

For QASUME data in Line 185-187:
"The measurements of direct solar spectral irradiance have a standard relative uncertainty of less than 1%, resulting in a standard uncertainty of 0.014 at 310 nm to 0.007 at longer wavelengths in AOD at an airmass of 1.5 (Gröbner et al. 2023)."

For BTS data in Line 195-197:
"An estimated expanded measurement uncertainty from 300 to 330 nm is within 3.5%, 330 to 450 nm is 1.9% and for the remaining spectral range it is 1.8 % (Gröbner et al. 2023)."

For RAman Lidar for Meteorological Observations (RALMO) data in Line 238-240:
"The estimated error in aerosol backscatter by RALMO at 355 nm for medium-high-aerosol-content data is $-0.018 \pm 0.237\ Mm^{-1}\ sr^{-1}$ and $+0.001 \pm 0.141\ Mm^{-1}\ sr^{-1}$ (+6 % ± 38 %) for altitudes 0.8–3 km a.s.l. and 0.8–6 km a.s.l., respectively (Brunamonti et al., 2021)."

For Ceilometer data in Line 243-244:
"The relative error in aerosol backscatter coefficient at 1064 nm is 10% (Wiegner and Geiss, 2012)."

2. For in situ measurement:

For Nephelometer data in Line 206-207:
"The measurement reproducibility for submicron data is within ± 1% while that for super micron data lies between 5-10% (Anderson and Ogren, 1998)."

For Aethalometer data in Line 210:
"The sensitivity of the absorption coefficient determination from AE33 to scattering is below 1-1.5%."

For aerodynamic particle sizer (APS) data in Line 216-217:
"The limits formed by the APS and Fidas size distributions around their averages were retained as an indication of the uncertainty in the merged size distributions above 0.6 μm diameter."

3. For satellite observation:

For MODIS data in Line 250-251:
"The global estimated error in the AOD retrieval for land is ± (0.05 + 20%) (Sayer et al., 2013, Sayer et al., 2019 and references there in)."

Regarding the discuss on the significance of the observed concave spectral curvature (AOD peak at ≈500 nm) with respect to the measurement uncertainties, we have added the following paragraph in Section 3.2.1 Lines 446-449:

"The mean (standard deviation), maximum and minimum values of the AOD difference (AOD at 500 nm – AOD at 340 nm) is found to be 0.21(0.07), 0.00, 0.34, respectively for HFX, 0.20 (0.07), 0.06, 0.29, respectively for BRT and, 0.05 (0.01), 0.02, 0.07, respectively for DAV. This indicates that the observed spectral curvature in AOD is significant in comparison to the measurement uncertainty in AOD (~0.01 in the visible and near infrared increasing to ~0.02 in the UV wavelengths)."

We have added the error bars in the key plots as suggested by the reviewer in the updated version of the manuscript.

Comment #5: The MODIS/MERRA-2 vs. AERONET comparisons in Appendix Table A3 should be interpreted with caution, since satellite algorithms are generally based on only 1 or 2 wavebands radiance inversion, while MERRA-2's spectral and microphysical properties are model-driven and constrained primarily by satellite column AOD at limited wavelengths with simplified microphysics. These approaches are not as likely to represent the peak around 500nm in observed AOD in-situ, and likely will not be captured in these datasets. While such comparisons are useful to show whether the event is represented in the reanalysis, they do not constitute independent validation of the aerosol size distribution, composition, or unusual spectral curvature observed. Several recent studies have shown that MERRA-2 and CAMS can underestimate absorbing aerosol loadings, that they miss key hotspot regions and underestimate BC by a substantial margin (Li et al., 2023; Liu Z et al., 2024). Including a brief discussion of these known limitations supporting the argument with similar findings elsewhere (Liu Z et al., 2024; Tiwari et al., 2025) would help contextualize the differences observed here and prevent over-interpretation of the agreement or disagreement with MERRA-2.

Response #5: We agree with the reviewer and are thankful for this suggestion. In order to avoid over-interpretation in Section 3.3, we have modified the following paragraph in Line 621-641 as below

"Several studies have shown that MERRA2 can substantially underestimate absorbing aerosol loadings (Shang et. al., 2024; Liu et al., 2024; Ceamanos et. al., 2023; Li et al., 2023).

AERONET has been used in various studies to evaluate MODIS AOD data and MODIS AOD uncertainty is defined based on this comparison (Sayer et al., 2013 and references there in). However, based on the results of Sayer et al. (2013), there are differences due to various reasons, including spatial comparison aspects, retrieval aspects etc. In addition, the vast majority of these data represent cases with relatively low AOD values. It is evident from Fig. 10 that for various stations the agreement of MODIS and AERONET AOD at the days affected by Canadian smoke differ from other days. This analysis suggests that in special cases, the defined uncertainties of satellite observations based on statistical differences with ground-based measurements may vary.

The comparisons made in this section are to see how well the event is represented in the satellite observations or model reanalysis, however, it does not constitute the validation of the aerosol properties retrieval or observed unusual spectral curvature. It is known that the satellite algorithms are based on limited wavebands radiance inversion, while MERRA2's spectral and microphysical properties are model-driven

and constrained primarily by satellite column AOD at limited wavelengths with simplified microphysics. MODIS and MERRA2 are interconnected in a way that the MERRA2 involves assimilation from MODIS as well as other observations. However, there still can be differences in the AOD estimations from the two algorithms in such rare situations as is also evident that the two panels of Fig. 10 differ.

This analysis suggests that satellite algorithms and model reanalysis are not as likely to represent the peak around 500 nm in AOD as observed from ground-based remote sensing and in-situ measurements, and likely will not be captured in these datasets. This analysis illustrates the importance of experimental and ground-based measurements to capture such rare extreme weather events during which there can be significant underestimation and/or overestimation from satellite and model reanalysis datasets."

Specific Comments:

Comment #6: The absence of coarse mode despite large accumulation sizes is puzzling!! Could this indicate measurement limitations in detecting super-micron particles? Was the APS merging process validated for such extreme distributions?

Response #6: We thank the reviewer for this observation. The presence of large accumulation mode is obvious as this is the case of smoke plume transport. This sentence was aimed to highlight the presence of large accumulation mode as compared to low coarse mode. However, we agree that the sentence "absence of coarse mode" can be confusing. Therefore, we have modified its usage accordingly throughout the manuscript. To clarify further, this is not a measurement limitation. e.g., at DAV the coarse mode particle concentration is very low as it is a remote and relatively clean site (see Table 2 that shows that the coarse mode volume concentration at DAV was almost the same before, during and after the peak day of the smoke plume transport, however there was increase in the fine mode volume concentration during the smoke plume transport i.e., on 01 October 2023).

Regarding the APS merging process, we have added the following description,

"The limits formed by the APS and Fidas size distributions around their averages were retained as an indication of the uncertainty in the merged size distributions above 0.6 µm diameter"

Please refer to Response #2 for description about detailed description about the APS size distribution.

Comment #7: Could you clarify what configuration was adapted for Mie model simulation, do we assume, core-shell, external, BC fractal morphology? Have you tested core-shell mixing would modify your Mie results? The refractive indices are derived from AERONET? And are used for Mie model (Figure 9)

Response #7: The results presented in Fig. 9 are from the operational AERONET inversion products. The Mie modelling is performed by the authors for Fig. 5 i.e., from in situ measurements and not the columnar measurements by sun photometers (i.e., AERONET measurements).

As explained in our response to the similar comment by the reviewer (comment and response #3) that was raised above, we have added additional discussion to Section 3.1.3 to explain why we use the homogeneous sphere assumption in our Mie theory calculation, and why we had no need to test other models with more explicit representations of BC aggregates in order to capture the absorption profiles better. We have also

modified the text in the caption of Fig. 5 (see above) as well as the following text in Section 3.1.3 to highlight that the homogeneous sphere model assumes a single, effective refractive index for all particles, which we indeed to took from the AERONET retrieval.

"All particles were assumed to be identical homogeneous spheres (except for their diameter), i.e., all components including BC and BrC were assumed to be present as homogeneous internal mixture with a single, effective refractive index. The polydisperse size distribution was constrained MPSS and APS in situ data, and the complex refractive index was taken from DAV AERONET retrieval results".

Comment #8: Does the plume's vertical evolution suggest lofting mechanisms beyond advection? How does the Fall seasonality potentially differentiate this from summer smoke events?

Response #8: Yes, the vertical evolution of wildfire plumes can have lofting mechanisms beyond simple advection, including intense convection and a solar heating-driven "self-lofting" process. While advection i.e., the transport of smoke by the mean horizontal wind is the primary driver of downwind smoke movement, it does not explain the extreme vertical rise often observed in large, high-intensity fires. The smoke plume transport in the current manuscript can be a case of pyrocumulonimbus formation as the plume layer was visible in MODIS true color images above the presence of clouds as can be seen from Appendix Fig. A2. The analysis related to pyrocumulonimbus formation is out of the scope of this manuscript. However, we have mentioned this in Line 548-552 as

"Another point to note in this smoke plume transport is that the fire plume was visible in the MODIS true colour images (Fig. A2 in Appendix) even in the presence of clouds which indicates that the injection height of this Canadian wildland fire was quite high. Zhang et. al. (2024) confirmed high pyrocumulonimbus (pyroCb) activity (a cumulonimbus clouds formed by wildfires-driven convection) activity during the Canadian wildfire season of 2023; however, only a minor amount of aerosol managed to reach above the troposphere, with most convective events limited to the upper troposphere."

Regarding the Fall seasonality, some of the similar AOD curvature or blue/green sun observation events that were recorded in September are Wilson 1951, Eck et al., 2023, and the current manuscript. However, the narrow and large particle size distribution have also been observed for months other than September e.g., Fiebig et al., 2003. However, we have removed the word "Fall" from the title as the observations presented in this manuscript are only for about a week and are not representative of the entire fall season.

Accordingly, we have modified the following Lines 699-704 in the conclusion section

"Another observation associated with the occurrence of this phenomenon is whether there can be some relation with the fire source such as fuel type, specific meteorological conditions, etc. as the event reported here occurred towards the end of September 2023 associated with Canadian wildfires as well as the event of California/Oregon fires presented by Eck et al., 2023 occurred in September of 2020 and the Alberta wildfire transport to Edinburgh as reported by Wilson 1951 occured in September 1950 (all these events are related to the wildfires in North America). However, the narrow and large particle size distribution have also been observed for months other than September e.g., Fiebig et al., 2003."

Comment #9: Were ACSM composition data used to constrain the AERONET inversions? How does the 500 nm AOD peak impact AERONET's size distribution retrieval accuracy?

Response #9: The AERONET inversions used in this manuscript is from official operational AERONET product. Regarding in situ measurements, details are provided in Response #2.

It is not possible to say anything about the retrieval uncertainty of peak AOD at 500 nm on AERONET inversions as AERONET inversions does not provide retrievals at 500 nm but are based on the sky scan radiance measurements at 340 nm, 440 nm, 675 nm and 870 nm. We have provided this information in Line 154-155 as

"The AERONET inversion products are based on the sky scan radiance measurements at 340 nm, 440 nm, 675 nm and 870 nm."

Comment #10: Clarify "smoke age" definition— Table 1 and its use (how days were assigned) should include the assumptions and uncertainties in age estimates (transport time ranges).

Response #10: We thank the reviewer for noticing this. We have removed the column of smoke age from Table 1 as it has not been used in interpretations throughout the manuscript.

Comment #11: Figure 6: Label station codes in subplots for clarity.

Response #11: We thank the reviewer for the comment. We have provided the station label codes in each subplot following the plot number e.g., (a1) HFX and so on. The station label description is provided in Table 1. The codes provided in Table 1 are used throughout the manuscript. We have added the following in the Figure caption in Line 423

"Station label description is provided in Table 1."

Comment #12: Figure 9: Include error bars for AERONET retrievals (SSA/RI uncertainties)

Response #12: We thank the reviewer for this suggestion. We have added error bars to Fig. 9 in the updated version of the manuscript.

References:

Anderson, T. L., Ogren, J. A. Determining Aerosol Radiative Properties Using the TSI 3563 Integrating Nephelometer, Aerosol Sci. Tech., 29:57– 69, doi:10.1080/02786829808965551, 1998.

Brunamonti, S., Martucci, G., Romanens, G., Poltera, Y., Wienhold, F. G., Hervo, M., Haefele, A., and Navas-Guzmán, F.: Validation of aerosol backscatter profiles from Raman lidar and ceilometer using balloon-borne measurements, Atmos. Chem. Phys., 21, 2267–2285, doi:10.5194/acp-21-2267-2021, 2021.

Chauvigné, A., Aliaga, D., Sellegri, K., Montoux, N., Krejci, R., Močnik, G., Moreno, I., Müller, T., Pandolfi, M., Velarde, F., Weinhold, K., Ginot, P., Wiedensohler, A., Andrade, M., and Laj, P.: Biomass burning and urban emission impacts in the Andes Cordillera region based on in situ measurements from the Chacaltaya observatory, Bolivia (5240 m a.s.l.), Atmos. Chem. Phys., 19, 14805–14824, doi:10.5194/acp-19-14805-2019, 2019.

Collaud Coen, M., Weingartner, E., Schaub, D., Hueglin, C., Corrigan, C., Henning, S., Schwikowski, M., and Baltensperger, U.: Saharan dust events at the Jungfraujoch: detection by wavelength dependence of the single scattering albedo and first climatology analysis, Atmos. Chem. Phys., 4, 2465–2480, doi:10.5194/acp-4-2465-2004, 2004.

Dubovik, O., Smirnov, A., Holben, B., King, M. D., Kaufman, Y. J., Eck, T. F., and Slutsker, I.: Accuracy assessments of aerosol optical properties retrieved from Aerosol Robotic Network (AERONET) Sun and sky radiance measurements, J. Geophys. Res., 105, 9791–9806, doi:10.1029/2000JD900040, 2000.

Eck, T. F., B. N. Holben, J. S. Reid, O. Dubovik, A. Smirnov, N. T. O'Neill, I. Slutsker, and S. Kinne (1999), Wavelength dependence of the optical depth of biomass burning, urban, and desert dust aerosols, J. Geophys. Res., 104(D24), 31333–31349, doi:10.1029/1999JD900923.

Eck, T. F., Holben, B. N., Reid, J. S., Sinyuk, A., Giles, D. M., Arola, A., Slutsker, I., Schafer, J. S., Sorokin, M. G., Smirnov, A., LaRosa, A. D., Kraft, J., Reid, E. A., O'Neill, N. T., Welton, E. J., Menendez, A. R.: The extreme forest fires in California/Oregon in 2020: Aerosol optical and physical properties and comparisons of aged versus fresh smoke, Atmos. Environ., 305, 119798, doi:10.1016/j.atmosenv.2023.119798, 2023.

Fiebig, M., Stohl, A., Wendisch, M., Eckhardt, S., and Petzold, A.: Dependence of solar radiative forcing of forest fire aerosol on ageing and state of mixture, Atmos. Chem. Phys., 3, 881–891, doi:10.5194/acp-3-881-2003, 2003.

Gröbner, J., Kouremeti, N., Hülsen, G., Zuber, R., Ribnitzky, M., Nevas, S., Sperfeld, P., Schwind, K., Schneider, P., Kazadzis, S., Barreto, Á., Gardiner, T., Mottungan, K., Medland, D., and Coleman, M.: Spectral aerosol optical depth from SI-traceable spectral solar irradiance measurements, Atmos. Meas. Tech., 16, 4667–4680, doi:10.5194/amt-16-4667-2023, 2023.

Kaskaoutis, D.G., Grivas, G., Stavroulas, I., Liakakou, E., Dumka, U.C., Gerasopoulos, E., Mihalopoulos, N.: Effect of aerosol types from various sources at an urban location on spectral curvature of scattering and absorption coefficients, Atmos. Res., 264, 105865, doi:10.1016/j.atmosres.2021.105865, 2021.

Kazadzis, S., Kouremeti, N., Nyeki, S., Gröbner, J., and Wehrli, C.: The World Optical Depth Research and Calibration Center (WORCC) quality assurance and quality control of GAW-PFR AOD measurements, Geosci. Instrum. Method. Data Syst., 7, 39–53, doi:10.5194/gi-7-39-2018, 2018a.

Li, J., Carlson, B. E. and Lacis, A. A., Using single-scattering albedo spectral curvature to characterize East Asian aerosol mixtures. J. Geophys. Res. Atmos., 120: 2037–2052, doi:10.1002/2014JD022433, 2015.

Sayer, A. M., N. C. Hsu, C. Bettenhausen, and M.-J. Jeong, Validation and uncertainty estimates for MODIS Collection 6 “Deep Blue” aerosol data, J. Geophys. Res. Atmos., 118, 7864–7872, doi:10.1002/jgrd.50600, 2013.

Sayer, A. M., Hsu, N. C., Lee, J., Kim, W. V., & Dutcher, S. T. Validation, stability, and consistency of MODIS collection 6.1 and VIIRS version 1 Deep Blue aerosol data over land. Journal of Geophysical Research: Atmospheres, 124, 4658–4688, doi:10.1029/2018JD029598, 2019.

Sinyuk, A., Holben, B. N., Eck, T. F., Giles, D. M., Slutsker, I., Korkin, S., Schafer, J. S., Smirnov, A., Sorokin, M., and Lyapustin, A.: The AERONET Version 3 aerosol retrieval algorithm, associated uncertainties and comparisons to Version 2, Atmos. Meas. Tech., 13, 3375–3411, doi:10.5194/amt-13-3375-2020, 2020.

Wiegner, M. and Geiß, A.: Aerosol profiling with the Jenoptik ceilometer CHM15kx, Atmos. Meas. Tech., 5, 1953–1964, doi:10.5194/amt-5-1953-2012, 2012.

Wilson, R.: The blue sun of 1950 September. Mon. Not. Roy. Astron. Soc. 111 (5), 478–489, doi:10.1093/mnras/111.5.478, 1951.

Yus-Díez, J., Bernardoni, V., Močnik, G., Alastuey, A., Ciniglia, D., Ivančič, M., Querol, X., Perez, N., Reche, C., Rigler, M., Vecchi, R., Valentini, S., and Pandolfi, M.: Determination of the multiple-scattering correction factor and its cross-sensitivity to scattering and wavelength dependence for different AE33 Aethalometer filter tapes: a multi-instrumental approach, Atmos. Meas. Tech., 14, 6335–6355, doi:10.5194/amt-14-6335-2021, 2021.

We thank the reviewer for the comments and suggestions that have helped us improve the quality of this manuscript.

Response to reviewer 2 comments

This study exploits multi-site, ground-based remote sensing instrumentation to provide a systematic analysis of the long-range transport, microphysical and optical properties of smoke from the 2023 Canadian wildfires that reached Europe in autumn. Uncommon spectral signatures of both AOD and SSA were identified across the ultraviolet-to-shortwave-infrared range (300–2200 nm), revealing previously unreported wavelength-dependent features in the aging smoke plume over Europe. The topic is highly relevant to ongoing extreme wildfire events within the context of global climate change and offers valuable insights for regional air-quality and climate-feedback studies. However, there are still some problems that need to be solved. Minor revisions are recommended before final acceptance.

Specific Comments:

Comment #1: Section 2 Data and Methodology, 2.1-2.4, The current section is poorly structured: it alternates between aerosol-property-based and instrument-platform–based sub-divisions, making the narrative difficult to follow.

Response #1: We thank the reviewer for this observation. Accordingly, we have re-structured Section 2 as below in the updated manuscript.

2.1 Ground based measurements

- 2.1.1 Aerosol columnar property measurements
- 2.1.2 Aerosol in situ measurements
- 2.1.3 Aerosol vertical profiles

2.2 Satellite observations

2.3 Aerosol trajectory modelling and model reanalysis

Additionally, we have renamed the Section 2 as "Data" to fit better with the narrative.

Comment #2: MODIS DT provide AOD over ocean and land, DB provides AOD over ocean, so for this study, which AOD is used here? What is the uncertainty of the dataset?

Response #2: We have provided the information regarding the use of MODIS AOD from both DT and DB algorithms as the plumes from the North America (land) reached Europe (land) via transport over the Atlantic Ocean (ocean) and have added the information related to uncertainty associated with the dataset in Section 2.2 Lines 246-251 in the updated manuscript as

"Satellite observation of AOD was obtained from the daily retrievals of the MODerate resolution Imaging Spectroradiometer (MODIS) Collection 6.1. MODIS Level 2 AOD retrievals at 550 nm (Levy et al., 2013; Wei et al., 2019b) from the Dark Target (DT) retrieval algorithm provide AOD values above ocean and land while the Deep Blue (DB) retrieval algorithms provides AOD values above land (used in Appendix Fig. A4). For the analysis presented in Section 3.3, MODIS DT AOD is used which is coincident with the AERONET stations. The global estimated error in the AOD retrieval for land is ± (0.05 + 20%) (Sayer et al., 2013, Sayer et al., 2019 and references there in)."

Comment #3: In the section 3.1.3, please give definition of SAE, AAE and SSA AE with the equation.

Response #3: We thank the reviewer for this suggestion following which we have added a new text section in the appendix to include these definitions and equations. The new appendix is referred to in the main text and copied here:

Appendix A, Section A1 as

"A1: Optical variables calculated from the in situ aerosol measurements

Light scattering coefficients were measured at three wavelengths ($\sigma_{sp}(\lambda)$ for $\lambda = 450, 550, 700$ nm) with an integrating nephelometer (TSI 3563). Light absorption coefficients were measured at seven wavelengths ($\sigma_{ap}(\lambda)$ for $\lambda = 370, 470, 520, 590, 660, 880, 950$ nm) with an absorption photometer (MAGEE scientific AE33). The scattering coefficient measurements are considered to have uncertainties of 10% (Anderson et al., 1996), while those of the absorption coefficients are considered to be 30% (Müller et al., 2011).

Scattering and absorption Ångström exponents (SAE and AAE values, respectively) were calculated pairwise between coefficients measured at two different wavelengths (λ_1 and λ_2) using the general Ångström exponent (AE) equation:

$$AE(\lambda_1\_\lambda_2) = \frac{\ln\left(\sigma(\lambda_1)/\sigma(\lambda_2)\right)}{\ln\left(\lambda_1/\lambda_2\right)} \quad . \qquad \text{(Eq. A1)}$$

The measured absorption coefficients were evaluated at the nephelometers wavelengths (i.e., $\sigma_{ap}(\lambda)$ for $\lambda = 450, 550, 700$nm were calculated) using the AAE values corresponding to the aethalometer wavelength pairs that bound each of the nephelometers wavelengths.

Single scattering albedo (SSA) values were calculated at the three nephelometer wavelengths ($\lambda = 450, 550, 700$nm) using the equation:

$$SSA(\lambda) = \frac{\sigma_{sp}(\lambda)}{(\sigma_{ap}(\lambda) + \sigma_{sp}(\lambda))} \quad . \qquad \text{(Eq. A2)}$$

Pairwise SSA Ångström exponents (SSA_AAE values) were calculated between the SSA values at two different wavelengths (λ_1 and λ_2) using Eq. A1.

Comment #4: Line 373, there are many stations only has one time stamp, how can say "all stations showed a greatly shifted peak …", for other station, the shift is also not obviously.

Response #4: We agree with the reviewer here. Therefore, we have removed this line from the manuscript in the updated version.

Comment #5: Section3.3 satellite observation and model evaluation are ancillary checks on the event. However, they are scarcely mentioned in the Abstract and Conclusions. The necessity of this section therefore needs to be further clarified.

Response #5: We agree with reviewer. We have included the statements about the satellite observations and model evaluation in the abstract and conclusion actions as mentioned below in the updated version of the manuscript.

Abstract, Line 29-31: The comparison of the Aerosol Robotic Network observations with satellite observation and model reanalysis showed an AOD underestimation ranging from 0.1 to 1.5.

Conclusion, Line 693-698: "The comparison of AERONET AOD with MODIS satellite based AOD retrievals for long range transported smoke plume showed a difference of approximately 0.4 that can be due to inhomogeneity within a pixel, ground reflectance, high altitude or presence of high absorption layer e.g., in this case was thick smoke plume. The comparison of AEROENT AOD with MERRA2 model reanalysis based AOD showed underestimation in most of the cases ranging from 0.1 to 1.5. This analysis highlights that it can be quite challenging for the satellite algorithms and model reanalysis to have complementary AOD retrievals in such rare extreme weather events that are captured by experimental and ground-based measurements."

Technical correction:

Comment #6: Figure 5, numbering in the figure caption and the citations within the text are inconsistent. Please verify and update accordingly.

Response #6: We thank the reviewer for identifying this error. We have corrected this discrepancy in the updated manuscript in Section 3.1.3.

Comment #7: Line134, refractive indices (RI) à refractive index, which is shown in the title 3.1.3

Response #7: It has been corrected to "refractive index" in Line 154 in the updated manuscript.

Comment #8: Line152, what is QASUME?

Response #8: the abbreviation "QASUME" has been expanded as "Quality Assurance of Spectral Ultraviolet Measurements" in Line 178 in the updated manuscript.

Comment #9: Line91, PM2.5 to $PM_{2.5}$

Response #9: corrected.

Comment #10: Line 250-251, change the order, 30 September first then 01 October

Response #10: corrected.

Comment #11: Figure 2, Please use the same y-axis legend for both panels (a) and (b).

Response #11: corrected.

Comment #12: Figure 4, what does the shadow means?

Response #12: We thank the reviewer for this comment and apologize for this omission. The caption of Fig.4 has now been updated as follows in Line 351-353 in the updated manuscript:

"Figure 4: Particle (a) number and (b) volume size distributions measured in situ at JFJ before, during, and after the passage of the smoke plume. The shaded areas represent the region formed by the APS- and Fidas-

measured size distributions, which were averaged to calculate the merged size distributions at particle diameters > 600 nm".

Comment #13: Line 339, what is MSC?

Response #13: We thank the reviewer for mentioning this. We have provided the description of abbreviation "MSC" which refers to "mass scattering cross-section" in Line 394 in the updated manuscript at the first instance MSC is mentioned in Section 3.1.3 in the updated version of the manuscript.

References:

Anderson, T. l., Covert, D. s., Marshall, S. f., Laucks, M. l., Charlson, R. j., Waggoner, A. p., Ogren, J. a., Caldow, R., Holm, R. l., Quant, F. r., Sem, G. j., Wiedensohler, A., Ahlquist, N. a., and Bates, T. s.: Performance Characteristics of a High-Sensitivity, Three-Wavelength, Total Scatter/Backscatter Nephelometer, J. Atmos. Oceanic Technol., 13, 967–986, https://doi.org/10.1175/1520-0426(1996)013<0967:PCOAHS>2.0.CO;2, 1996.

Levy, R. C., Mattoo, S., Munchak, L. A., Remer, L. A., Sayer, A. M., Patadia, F., and Hsu, N. C.: The Collection 6 MODIS aerosol products over land and ocean, Atmos. Meas. Tech., 6, 2989–3034, doi:10.5194/amt-6-2989-2013, 2013.

Müller, T., Henzing, J. S., de Leeuw, G., Wiedensohler, A., Alastuey, A., Angelov, H., Bizjak, M., Collaud Coen, M., Engström, J. E., Gruening, C., Hillamo, R., Hoffer, A., Imre, K., Ivanow, P., Jennings, G., Sun, J. Y., Kalivitis, N., Karlsson, H., Komppula, M., Laj, P., Li, S.-M., Lunder, C., Marinoni, A., Martins dos Santos, S., Moerman, M., Nowak, A., Ogren, J. A., Petzold, A., Pichon, J. M., Rodriquez, S., Sharma, S., Sheridan, P. J., Teinilä, K., Tuch, T., Viana, M., Virkkula, A., Weingartner, E., Wilhelm, R., and Wang, Y. Q.: Characterization and intercomparison of aerosol absorption photometers: result of two intercomparison workshops, Atmos. Meas. Tech., 4, 245–268, https://doi.org/10.5194/amt-4-245-2011, 2011.

Sayer, A. M., N. C. Hsu, C. Bettenhausen, and M.-J. Jeong, Validation and uncertainty estimates for MODIS Collection 6 "Deep Blue" aerosol data, J. Geophys. Res. Atmos., 118, 7864–7872, doi:10.1002/jgrd.50600, 2013.

Sayer, A. M., Hsu, N. C., Lee, J., Kim, W. V., & Dutcher, S. T. Validation, stability, and consistency of MODIS collection 6.1 and VIIRS version 1 Deep Blue aerosol data over land. Journal of Geophysical Research: Atmospheres, 124, 4658–4688, doi:10.1029/2018JD029598, 2019.

Wei, J., Li, Z., Sun, L., Peng, Y., Wang, L.: Improved merge schemes for MODIS Collection 6.1 Dark Target and Deep Blue combined aerosol products, Atmos. Environ., 202, 315-327, doi:10.1016/j.atmosenv.2019.01.016, 2019.

We thank the reviewer for the comments and suggestions that have helped us improve the quality of this manuscript.

Response to reviewer 3 comments

This manuscript by Masoom et al. addresses an important and timely topic, presenting observational evidence of Canadian wildfire smoke transported across North America and Europe in fall 2023. The study highlights several unique aerosol characteristics, including concave spectral curvature in AOD, non-monotonic SSA, unusually large accumulation-mode particle sizes, and strong UV absorption indicative of brown carbon and/or tar balls. While the observations are compelling, several aspects of the manuscript require clarification or elaboration to strengthen scientific rigor and readability.

General comments:

Comment #1: The observed concave spectral curvature in AOD and SSA is very interesting. A more detailed discussion on the underlying physical mechanisms such as particle size distribution, mixing state, and the presence of absorbing organic aerosols (e.g., brown carbon) would enhance the manuscript's depth.

Response #1: We thank the reviewer for this suggestion. We have provided an extensive explanation for the unusual spectral dependence in Section 3.1.3 (e.g., please refer to the description for Fig. 5 in Lines 373-407). However, we agree that in the earlier version of the manuscript, there was a lack of clarity and to fix that we have added the following in the introduction Section 1 Lines 133-138 as

"Following the Introduction in Section 1, Section 2 presents an overview of the data used in this manuscript. Section 3 provides the description of the event as observed at the Swiss Alps using remote sensing and in situ measurements providing explanation of the event using in situ measurements in Section 3.1.3. Further Section 3.2 presents the tracing of the event using ground-based measurements (mainly remote sensing), ending with an explanation of the event from remote sensing measurements. Section 3 concludes with the satellite and model reanalysis based evaluation of the event. Finally, the manuscript findings are concluded in Section 4."

We have added the following description using remote sensing measurements to add further explanation as presented in Section 3.2.3 Lines 538-547 as below and in Fig 9e in the updated manuscript:

"In order to estimate the favorable physical parameters associated with the peak at 500 nm causing the observed concave spectral curvature in AOD, we looked into the role of refractive index, particle size, wavelength of incoming of incoming radiation on the extinction efficiency calculated from Mie scattering theory as presented in Fig. i (Fig. 9e in the updated manuscript) from remote sensing measurement (also in Fig. 5 with size distributions constrained by in situ measurements). The refractive index and the particle size are considered as presented in Fig. 6 and Fig. 9, respectively for HFX, BRT and DAV. For a refractive index in range 1.53-1.56, it is observed that for particle radius of 0.34 μm and wavelength varying from 340-500 nm, the extinction is found to decrease with increase in size parameter which is inversely relation with wavelength (i.e., extinction efficiency increases with wavelength). This direct proportionality of extinction efficiency to wavelength was found to be pertinent for the particle size above about 0.25 μm for submicron particles with refractive index varying in the range 1.53-1.56."

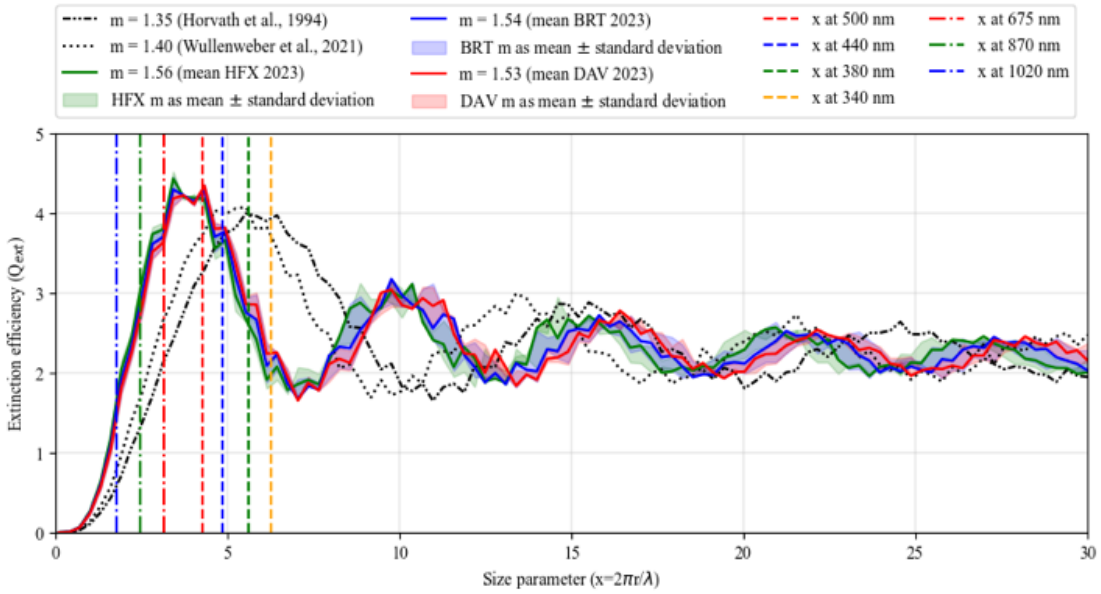

Figure i: Extinction efficiency for the observed refractive index at HFX, BRT and DAV, and size parameter at wavelength in the range 340-1020 nm from Mie scattering with homogeneous spherical particle assumption.

Comment #2: General suggestion/curiosity: it would be useful to compare the observed spectral features and particle properties with past wildfire smoke transport events at the same site to highlight what makes the 2023 episode unique. The authors also mention that seasonal factors may play a role; it is therefore important to compare these observations with past events.

Response #2: We are thankful for the reviewer for this suggestion. We have provided a climatological variation of the daily average spectral AOD variation at Davos as well as the daily peak AOD wavelength highlighted as black dots from 2004-2022 as shown in Fig ii below (Fig. A1 in the manuscript). Here, we have not restricted the analysis to only the wildfires cases but have performed this climatological analysis for all the available dataset during this time period.

Regarding the seasonality, some of the similar AOD curvature or blue/green sun observation events were recorded in September are Wilson 1951, Eck et al., 2023, and the current manuscript. However, the narrow and large particle size distribution have also been observed for months other than September e.g., Fiebig et al., 2003. Hence, we have removed the word "Fall" from the title as the observations presented in this manuscript are only for about a week and are not representative of the entire fall season. Accordingly, we have modified the following Lines 699-704 in the conclusion section

"Another observation associated with the occurrence of this phenomenon is whether there can be some relation with the fire source such as fuel type, specific meteorological conditions, etc. as the event reported here occurred towards the end of September 2023 associated with Canadian wildfires as well as the event of California/Oregon fires presented by Eck et al., 2023 occurred in September of 2020 and the Alberta wildfire transport to Edinburgh as reported by Wilson 1951 occured in September 1950 (all these events are related to the wildfires in North America). However, the narrow and large particle size distribution have also been observed for months other than September e.g., Fiebig et al., 2003."

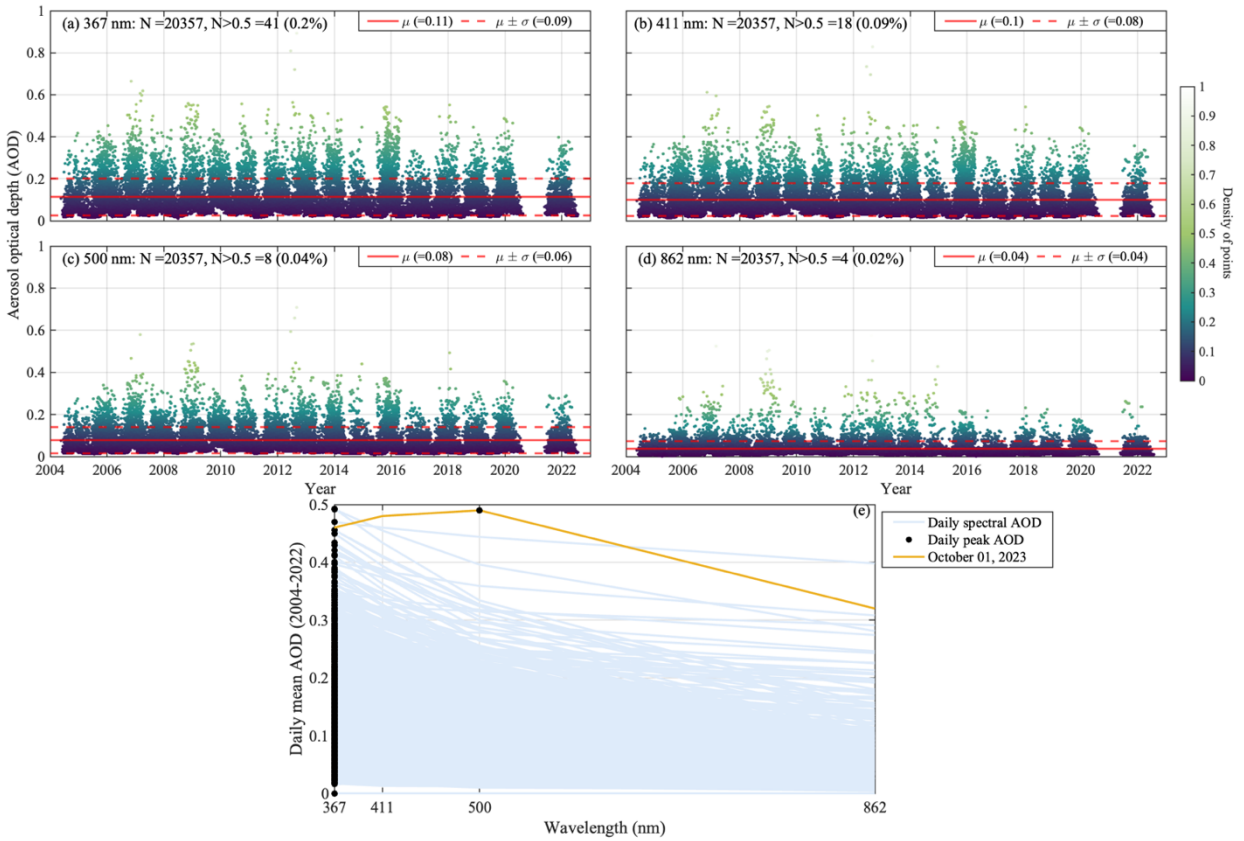

Figure A1: (a-d) Climatological AOD variation at 367, 411, 500 and 862 nm and, (e) Daily mean spectral AOD and (e) daily spectral maxima (black dots) between 2004-2022 from GAWPFR 01 October 2023 (yellow) at DAV

Specific comments:

Comment #3: L82: -> et al. (2024)

Response #3: corrected.

Comment #4: L92: PM2.5 -> PM2.5

Response #4: corrected.

Comment #5: L137-L139: why not Level 2 AERONET data with improved quality?

Response #5: We have updated the AERONET data used in this analysis from Level 1.5 to Level 2.0. However, it has not changed the analysis. Hence, we chose to use Level 2.0 dataset and wherever Level 2.0 is not available, we have used Level 1.5 (We have mentioned this throughout the manuscript wherever Level 1.5 dataset has been used) as well as have provided this description in Section 2.1.1 Lines 148-164 as below,

“Level 2.0 AERONET data have been utilized for several stations for tracing the plume as presented in Section 3.2. The AERONET field instruments are inter-calibrated at Mauna Loa and Izana Langley calibrated reference instruments resulting in AOD uncertainty at optical airmass 1 of ~0.01 in the visible and near infrared increasing to ~0.02 in the UV wavelengths (Eck et al. 1999). AERONET inversion products from level 2.0 and level 1.5 (level 1.5 is used only when level 2.0 data is not available and an additional criterion is used in this case to filter the data as described below) have also been utilised in this work including single scattering albedo (SSA), absorption aerosol optical depth (AAOD), absorption Ångström exponent (AAE), volume size distribution (VSD) and refractive index (RI). The nominal uncertainty in AERONET SSA for AOD at 440 nm above 0.40 is ~0.03 and the SSA uncertainty decreases with increase in AOD (Dubovik et al., 2000; Sinyuk et al., 2020). The estimated uncertainty for real refractive index is well below 0.04 for AOD greater than 0.5 for biomass burning cases (Dubovik et al., 2000; Sinyuk et al., 2020). The uncertainty in volume median radius is estimated to be 0.1\pm0.5 % and 5.4\pm4 % for fine and coarse mode, respectively (it is an indication of good confidence in size distribution retrievals) (Sinyuk et al., 2020). The absorption AOD values as reported in the AERONET almucantar inversion dataset are obtained using the relationship AAOD=(1−SSA) ×AOD. A detailed uncertainty estimation of AERONET inversion product for version 3 can be found at Sinyuk et al. (2020). For the analysis in this manuscript, we have used the AERONET inversion products Level 2.0 and Level 1.5 (with sky error below 5% and solar zenith angle above 45° and the coincident AOD values at 440 nm above 0.40).”

Comment #6: Section 2: Since multiple aerosol data sources are used, it would strengthen the manuscript to discuss the uncertainties associated with each dataset (e.g., remote sensing retrievals, in situ measurements) and how these uncertainties might propagate into the subsequent analysis. This would provide readers with a clearer understanding of the confidence in the results.

Response #6: We thank the reviewer for this suggestion. We have added uncertainty information associated with the dataset used in this manuscript in Section 2.1.1 as below,

1. For remote sensing retrievals:

For AERONET data in Line 149-164:
“The AERONET field instruments are inter-calibrated at Mauna Loa and Izana Langley calibrated reference instruments resulting in AOD uncertainty at optical airmass 1 of ~0.01 in the visible and near infrared increasing to ~0.02 in the UV wavelengths (Eck et al. 1999). The nominal uncertainty in AERONET SSA for AOD at 440 nm above 0.40 is ~0.03 and the SSA uncertainty decreases with increase in AOD (Dubovik et al., 2000; Sinyuk et al., 2020). The estimated uncertainty for real refractive index is well below 0.04 for AOD greater than 0.5 for biomass burning cases (Dubovik et al., 2000; Sinyuk et al., 2020). The uncertainty in volume median radius is estimated to be 0.1±0.5 % and 5.4±4 % for fine and coarse mode, respectively (it is an indication of good confidence in size distribution retrievals) (Sinyuk et al., 2020). The absorption AOD values as reported in the AERONET almucantar inversion dataset are obtained using the relationship AAOD=(1−SSA) ×AOD. A detailed uncertainty estimation of AERONET inversion product for version 3 can be found at Sinyuk et al. (2020). For the analysis in this manuscript, we have used the AERONET

inversion products Level 2.0 and Level 1.5 (with sky error below 5% and solar zenith angle above 45° and the coincident AOD values at 440 nm above 0.40)"

For GAWPFR data in Line 169-170:
"Instruments are calibrated yearly or in 2 years on the basis of instrumental and logistic aspects and the calibration uncertainty is assured to be within ±1% (Kazadzis et al., 2018a)."

For QASUME data in Line 185-187:
"The measurements of direct solar spectral irradiance have a standard relative uncertainty of less than 1%, resulting in a standard uncertainty of 0.014 at 310 nm to 0.007 at longer wavelengths in AOD at an airmass of 1.5 (Gröbner et al. 2023)."

For BTS data in Line 195-197:
"An estimated expanded measurement uncertainty from 300 to 330 nm is within 3.5%, 330 to 450 nm is 1.9% and for the remaining spectral range it is 1.8 % (Gröbner et al. 2023)."

For RAman Lidar for Meteorological Observations (RALMO) data in Line 238-240:
"The estimated error in aerosol backscatter by RALMO at 355 nm for medium-high-aerosol-content data is $-0.018 \pm 0.237\ Mm^{-1}\ sr^{-1}$ and $+0.001 \pm 0.141\ Mm^{-1}\ sr^{-1}$ (+6 % ± 38 %) for altitudes 0.8–3 km a.s.l. and 0.8–6 km a.s.l., respectively (Brunamonti et al., 2021)."

For Ceilometer data in Line 243-244:
"The relative error in aerosol backscatter coefficient at 1064 nm is 10% (Wiegner and Geiss, 2012)."

2. For in situ measurement:

For Nephelometer data in Line 206-207:
"The measurement reproducibility for submicron data is within ± 1% while that for super micron data lies between 5-10% (Anderson and Ogren, 1998)."

For Aethalometer data in Line 210:
"The sensitivity of the absorption coefficient determination from AE33 to scattering is below 1-1.5%."

For aerodynamic particle sizer (APS) data in Line 216-217:
"The limits formed by the APS and Fidas size distributions around their averages were retained as an indication of the uncertainty in the merged size distributions above 0.6 μm diameter."

3. For satellite observation:

For MODIS data in Line 250-251:
"The global estimated error in the AOD retrieval for land is ± (0.05 + 20%) (Sayer et al., 2013, Sayer et al., 2019 and references there in)."

Comment #7: Section 2 Data and Methodology: Consider renaming the section to simply “Data”, as this may more accurately reflect the content.

Response #7: We agree with the reviewer and have modified the title of Section 2 as “Data” in Line 139 in the updated manuscript.

Comment #8: Figure A1e: the label (e) appears to be blocked, please readjust it.

Response #8: Corrected.

Comment #9: Section 3.1.3: what about the AERONET derived SD, SSA and CRI?

Response #9: We thank the reviewer for this comment. This section deals with the in situ measurements. Accordingly, for appropriate interpretation, we have modified the Section title as

“3.1.3 Sensitivity of AOD spectral dependence to aerosol particle size distribution, mixing state, refractive index and shape at Jungfraujoch from in situ measurements”

AERONET derived SD, SSA and CRI are discussed in Section 3.2.

Comment #10: Specific comment on Section 3.1.2 – “Anomalous spectral aerosol optical properties at Davos and Jungfraujoch”: Please consider to include a comparison with prior biomass burning events (2004–2022) to better contextualize the observed AOD values exceeding 0.5 and the spectral peak around 500 nm. The authors should expand the discussion on possible causes of this unusual spectral curvature, including particle size distribution, mixing state, and the presence of absorbing organics such as brown carbon. Providing the temporal evolution of spectral AOD at sub-daily resolution would help assess whether the observed anomaly is transient or sustained.

Response #10: We have performed a climatological analysis at Davos from the 20 years of available AOD data from PFR as presented in Fig. A1. Please refer to Response #2 for detailed description. For this analysis, we have not restricted the analysis only to wildfires, but have looked into the entire AOD dataset to spot the spectral peak around 500 nm.

We have tried to provide the physical mechanism that relates to the observed concave spectral curvature in AOD details of which has been provided in Response #1.

We have provided the temporal evolution of the spectral AOD at sub-daily scale as presented in Fig. i (Fig. 2 in the updated manuscript) below. The related description has been added to Lines 297-299 as below,

“The temporal evolution of the spectral curvature in AOD as presented in Fig. 2 (c, d) shows that at JFJ, the peak at 500 nm was prevalent during morning time of 30 September 2023 while at DAV, the peak at 500 nm was prevalent through the entire day (01 October 2023).”

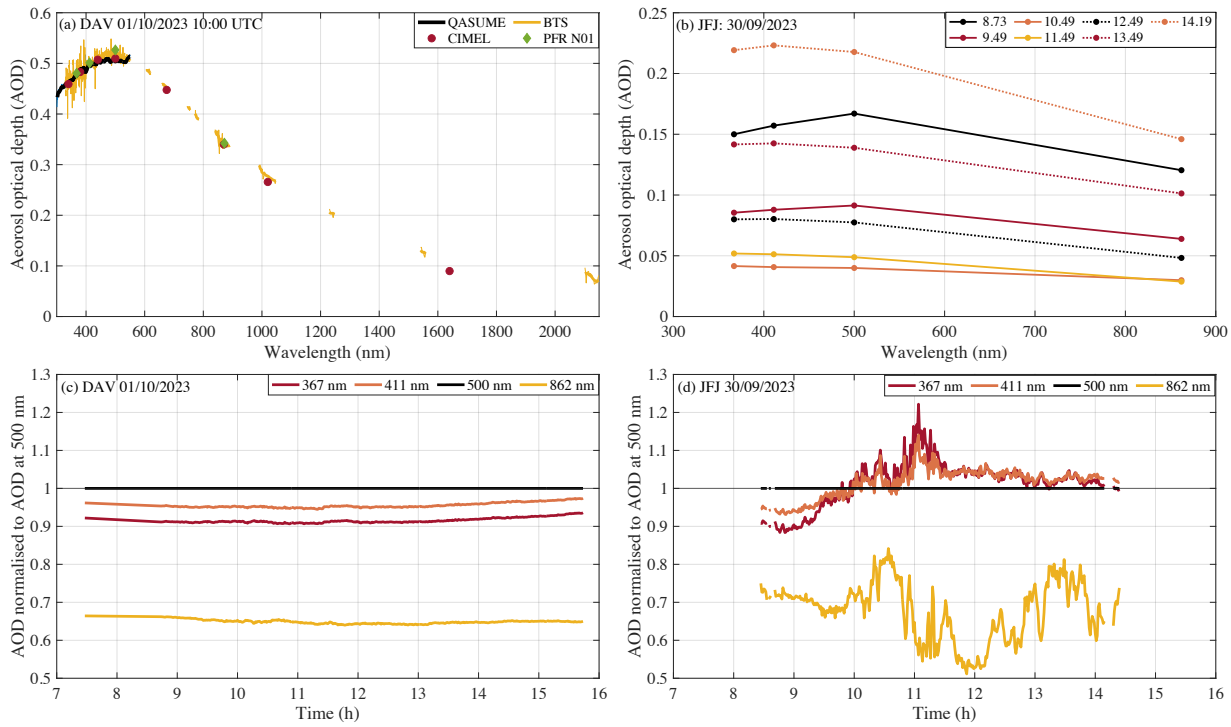

Figure i: (a) Instantaneous spectral AOD variation at 10:00 UTC in DAV on 01/10/2023 from sun photometer (Cimel and PFR) and spectroradiometer (BTS and QASUME). (b) Spectral AOD variation at JFJ on 30/09/2023 from PFR calculated as mean with 1 h time stamp for the whole day (time represented in the legend in UTC). (c, d) Temporal evolution of the AOD normalised to AOD at 500 nm at DAV and JFJ, respectively at sub-daily resolution.

Comment #11: Specific comment on Section 3.2.1 – "High aerosol loading and unique spectral AOD curvature": I would suggest to provide a more detailed discussion of the physical mechanisms underlying the observed AOD curvature across different stations. The link between the observed shift in the volume size distribution (VSD) fine-mode peak (~800 nm) and the spectral curvature in AOD should be clarified, including potential retrieval limitations under high aerosol loading. Furthermore, the criteria used to define "high AOD days" and spectral curvature events should be quantified.

Response #11: The addition of discussion on the probable cause and physical mechanism as pointed by the reviewer in Comment #1, #10 and #11, has been collectively provided in Response #1. The link between the shift in the size distribution, peak particle size and AOD curvature has been provided in Response #1.

Regarding the retrieval limitations, we have provided the required details as presented in Response #6.

Regarding the criterion of high AOD days and spectral curvature, we have added the following details in Section 3.2.1 Lines 414-416 as

"During the year 2023, AOD of the days exceeding 3 times the mean AOD of the respective site were selected as high AOD days. For these days, peak AOD occurring at wavelength other than 340 nm (minimum measurement wavelength) was used as the criterion for spectral curvature."

References:

Brunamonti, S., Martucci, G., Romanens, G., Poltera, Y., Wienhold, F. G., Hervo, M., Haefele, A., and Navas-Guzmán, F.: Validation of aerosol backscatter profiles from Raman lidar and ceilometer using balloon-borne measurements, Atmos. Chem. Phys., 21, 2267–2285, doi:10.5194/acp-21-2267-2021, 2021.

Anderson, T. L., Ogren, J. A. Determining Aerosol Radiative Properties Using the TSI 3563 Integrating Nephelometer, Aerosol Sci. Tech., 29:57– 69, doi:10.1080/02786829808965551, 1998.

Wiegner, M. and Geiß, A.: Aerosol profiling with the Jenoptik ceilometer CHM15kx, Atmos. Meas. Tech., 5, 1953–1964, doi:10.5194/amt-5-1953-2012, 2012.

Wilson, R.: The blue sun of 1950 September. Mon. Not. Roy. Astron. Soc. 111 (5), 478–489, doi:10.1093/mnras/111.5.478, 1951.

Eck, T. F., Holben, B. N., Reid, J. S., Sinyuk, A., Giles, D. M., Arola, A., Slutsker, I., Schafer, J. S., Sorokin, M. G., Smirnov, A., LaRosa, A. D., Kraft, J., Reid, E. A., O'Neill, N. T., Welton, E. J., Menendez, A. R.: The extreme forest fires in California/Oregon in 2020: Aerosol optical and physical properties and comparisons of aged versus fresh smoke, Atmos. Environ., 305, 119798, doi:10.1016/j.atmosenv.2023.119798, 2023.

Fiebig, M., Stohl, A., Wendisch, M., Eckhardt, S., and Petzold, A.: Dependence of solar radiative forcing of forest fire aerosol on ageing and state of mixture, Atmos. Chem. Phys., 3, 881–891, doi:10.5194/acp-3-881-2003, 2003.

Eck, T. F., B. N. Holben, J. S. Reid, O. Dubovik, A. Smirnov, N. T. O'Neill, I. Slutsker, and S. Kinne (1999), Wavelength dependence of the optical depth of biomass burning, urban, and desert dust aerosols, J. Geophys. Res., 104(D24), 31333–31349, doi:10.1029/1999JD900923.

Dubovik, O., Smirnov, A., Holben, B., King, M. D., Kaufman, Y. J., Eck, T. F., and Slutsker, I.: Accuracy assessments of aerosol optical properties retrieved from Aerosol Robotic Network (AERONET) Sun and sky radiance measurements, J. Geophys. Res., 105, 9791–9806, doi:10.1029/2000JD900040, 2000.

Sinyuk, A., Holben, B. N., Eck, T. F., Giles, D. M., Slutsker, I., Korkin, S., Schafer, J. S., Smirnov, A., Sorokin, M., and Lyapustin, A.: The AERONET Version 3 aerosol retrieval algorithm, associated uncertainties and comparisons to Version 2, Atmos. Meas. Tech., 13, 3375–3411, doi:10.5194/amt-13-3375-2020, 2020.

Sayer, A. M., N. C. Hsu, C. Bettenhausen, and M.-J. Jeong, Validation and uncertainty estimates for MODIS Collection 6 “Deep Blue” aerosol data, J. Geophys. Res. Atmos., 118, 7864–7872, doi:10.1002/jgrd.50600, 2013.

Sayer, A. M., Hsu, N. C., Lee, J., Kim, W. V., & Dutcher, S. T. Validation, stability, and consistency of MODIS collection 6.1 and VIIRS version 1 Deep Blue aerosol data over land. Journal of Geophysical Research: Atmospheres, 124, 4658–4688, doi:10.1029/2018JD029598, 2019.

Kazadzis, S., Kouremeti, N., Nyeki, S., Gröbner, J., and Wehrli, C.: The World Optical Depth Research and Calibration Center (WORCC) quality assurance and quality control of GAW-PFR AOD measurements, Geosci. Instrum. Method. Data Syst., 7, 39–53, doi:10.5194/gi-7-39-2018, 2018a.

Gröbner, J., Kouremeti, N., Hülsen, G., Zuber, R., Ribnitzky, M., Nevas, S., Sperfeld, P., Schwind, K., Schneider, P., Kazadzis, S., Barreto, Á., Gardiner, T., Mottungan, K., Medland, D., and Coleman, M.: Spectral aerosol optical depth from SI-traceable spectral solar irradiance measurements, Atmos. Meas. Tech., 16, 4667–4680, doi:10.5194/amt-16-4667-2023, 2023.

We thank the reviewer for the comments and suggestions that have helped us improve the quality of this manuscript.